Adjoint-Based Constrained Control of Eulerian Transportation Networks: Application to Air Traffic Control[†]

Alexandre M. Bayen[‖]   Robin L. Raffard[b]   Claire J. Tomlin[‖]

Abstract— We use an Eulerian network model of the airspace to simulate air traffic in congested areas of airspace. The model relies on a set of coupled first order hyperbolic partial differential equations (PDEs), obtained from the original Lighthill-Whitham-Richards (LWR) traffic model. The Jameson-Schmidt-Turkel (JST) is selected among other numerical schemes to perform simulations, and evidence of numerical convergence is assessed against known analytical solutions. Linear numerical schemes are discarded because of their poor performance, thus prohibiting the use of linear optimization for controlling the network. Instead, the adjoint problem of the linearized network control problem is computed. The constraints of the problem are enforced using a logarithmic barrier method. Simulations are run with real air traffic data to demonstrate the applicability of the method for traffic management. Scenarios involving several airports between Chicago and the East Coast are investigated.

I. INTRODUCTION

In a companion paper [3], we have described how to model the National Airspace System (NAS) using an Eulerian framework, inspired by the work of Menon et al. [15]. The result of this article was a model of airspace as a network of interconnected links, on which the aircraft density is governed by a set of first order hyperbolic *partial differential equations* (PDEs), coupled through boundary conditions. We validated this model and showed that it predicts accurate aircraft counts. In this paper, we first show how to apply standard numerical analysis tools to this system of PDEs, in order to perform numerical simulations when we do not have explicit analytical solutions available to us (which is the case in general). The major difficulty which we will show is that the solutions we construct are by essence discontinuous and have kinks, a very undesirable property for numerical solutions of PDEs. We also show that the use of linear numerical schemes to approximate the solution of the PDE perform very poorly, which unfortunately precludes the use of standard linear optimization programs to control the system.

‖ IEEE Member, Major (Ingénieur Principal de l'Armement), DGA, France. Autonomous Navigation Laboratory, LRBA, Vernon, France. Corresponding author. bayen@stanford.edu. Tel: (33-2)-27.24.41.87, Fax: (33-2)-27.24.44.99
b Ph.D. Student, Aeronautics and Astronautics, Stanford University.
‖ Assistant Professor, Aeronautics and Astronautics, Courtesy Assistant Professor, Electrical Engineering; Director, Hybrid Systems Laboratory, Stanford University.

Instead, we show thatwe may use flow control techniques [5], which are directly applicable to PDE-driven systems. We use an adjoint-based method, which enables us to compute the gradient of a cost function algebraically using the adjoint problem. We have to adapt the adjoint method to the case in which the system is described by a set of PDEs coupled through the boundary conditions, in presence of constraints. Unfortunately, this is a nonlinear control problem which does not provide proofs of convergence to a *global* optimal. However, this method, as well as other flow control approaches [11], [2], [1], [7], [13], have been shown to work extremely well in practice in fluid mechanics. In addition, though we consider networks of PDEs, the dimension of each PDE is one, enabling online implementations, as solving a set of one dimensional PDEs may be done extremely quickly. Controlling transportation networks in general is extremely challenging and numerically difficult [8], [16]. In the present case, the control consists in speed assignments and routing policies (i.e. determining optimal routes for the aircraft). As shown in [3], we use an *Eulerian* framework for this problem, despite the known difficulties inherent to PDE control [5], [1]. However, there are a few benefits of the above outlined approach over *Lagrangian* methods, which incorporate all trajectories of all aircraft:

1) Most of the Lagrangian methods will end up posing a control problem as an integer optimization program which is intractable in real time because it is NP-complete. In addition, the solution provided by these methods often takes advantage of actuating single aircraft individually, which precludes the derivation of global policies, which we are interested in for this paper. Finally, this framework scales very well with the number of aircraft (the higher the number of aircraft is the better the more accurate the model becomes, without further computational complexity).

2) The method presented below is very general and can be very easily adapted to specific classes of controllers, which are "Air Traffic Controller friendly", i.e. it is possible to use this method to derive a control law in a required format, which is compatible with aircraft capabilities.

3) This method can be applied to highway traffic with minor modifications [4], and we believe can be extended to other problems such as networks of irrigation channels [14].

This article is organized as follows. In Section II, we show the relative benefits of several numerical schemes, and run

tests against an analytical solution derived in [3]. We select the *Jameson-Schmidt-Turkel* (JST) scheme for the rest of this study. In Section III, we derive the adjoint system to our problem, and show how to use it to determine the mean velocity profiles along the links as well as the routing policy to apply. Finally, in Section IV, we show how to apply this to a very busy portion of airspace: the area enclosed by Chicago, New-York, Boston and the east coast of Canada.

N	number of links
S	set of source links
$\mathcal{M}$	set of links into which other links merge
$\mathcal{D}$	set of links ending in a fork
$\mathcal{U}(i)$	set of links merging into link i (if $i \in \mathcal{M}$)
$\mathcal{F}$	set of links merging into the airport (sink)
i_l, i_r	indices of the two links of a fork if link $i \in \mathcal{D}$
L_i	length of link i
x_i	arclength on link i: $x_i \in [0, L_i]$
$\rho_i(x_i, t)$	aircraft density on link i
$\rho_i^0(x_i)$	initial aircraft density on link i
$v_i(x_i)$	nominal velocity profile on link i: $v_i(\cdot) : [0, L_i] \to \mathbb{R}^+$
$q_i^{in}(t)$	inflow at $x_i = 0$ for link i (if applicable)
$\beta_i(t)$	portion of ρ_i which flows into link i_l (if applicable)

II. NUMERICAL SOLUTIONS AND VALIDATION

The Eulerian PDE model which we presented in the companion paper [3] is summarized as follows.

$$
\begin{cases}
\mathcal{N}_i(\rho_i) := \frac{\partial \rho_i(x_i,t)}{\partial t} + \frac{\partial}{\partial x_i}\left(\rho_i(x_i,t)v_i(x_i,t)\right) = 0 \\
\qquad\qquad\qquad\qquad\qquad\qquad\qquad\qquad \forall i \in \{1, \cdots, N\} \\
\rho_i(x,0) = \rho_i^0(x) \qquad\qquad\qquad\quad \forall i \in \{1, \cdots, N\} \\
\rho_i(0,t)v_i(0,t) = \sum_{j \in \mathcal{U}(i)} \rho_j(L_j,t)v_j(L_j,t) \qquad \forall i \in \mathcal{M} \\
\begin{cases} \rho_{i_l}(0,t)v_{i_l}(0,t) = \beta_i\,\rho_i(L_i,t)v_i(L_i,t) \\ \rho_{i_r}(0,t)v_{i_r}(0,t) = (1-\beta_i)\rho_i(L_i,t)v_i(L_i,t) \end{cases} \forall i \in \mathcal{D} \\
\rho_i(0,t)v_i(0,t) = q_i^{in}(t) \qquad\qquad\qquad\quad \forall i \in \mathcal{S}
\end{cases}
\tag{1}
$$

where notations are summarized in the table above. Please refer to [3] for more precision about the different variables used. In (1), $\mathcal{N}_i(\cdot)$ represents the LWR operator. Even for a single link i, it is in general not possible to solve the system (1) analytically. In [3], we show an analytical solution based on the method of characteristics, which works in the case in which $v_i(x_i, t) = v_i(x_i)$, i.e. the nominal velocity does not depend on time. When the velocity depends on time, numerical integration is needed. The solutions of the LWR PDE in the system (1) have very undesirable properties for numerical integrations: they are by construction discontinuous (see the construction of ρ_i in [3]); they can develop kinks if the velocity profiles are discontinuous. Ad hoc numerical schemes of the original LWR PDE have been the focus of recent research [9] in order to address similar difficulties encountered in the original LWR PDE; they have proved extremely efficient in the case of highway traffic. We have chosen to use three different schemes to compare their respective benefits.

1) The well known *Lax-Friedrichs scheme* [10]. This scheme is linear; we chose it motivated by the recent work [15], which make explicit use of the linearity of their discretization scheme in the control synthesis for their problem.

2) A *left-centered scheme*, inspired by the Daganzo scheme [9] in light traffic:
$$
\rho_k^{n+1} = \left(\rho_k^n(1 - \frac{c(x_k)\Delta T}{\Delta x}) + \rho_{k-1}^n(\frac{c(x_k)\Delta T}{\Delta x})\right) \times \left(1 - \frac{c(x_k)\Delta T}{\Delta x} + \frac{c(x_{k-1})\Delta T}{\Delta x}\right)
$$

3) The *Jameson-Schmidt-Turkel* (JST) *scheme*. This scheme is nonlinear, and has very desirable properties for this work: it captures shocks (which are present in the solutions we compute, as will be seen), and when the PDE has an entropy solution, which is the case for highway traffic in the original LWR setting, it converges to the entropy solution of the problem. Details of this scheme are available in [12].

Even if a numerical scheme is theoretically proved to converge to the analytical solution of a PDE, one usually does not know a priori the required gridsize to guarantee that the numerical solution is close to the analytical solution. Even if this type of validation is standard in numerical analysis [10], it seems to be absent from literature using these schemes for highway or air traffic problems [15], [9]. We use the method developed in [3] to compute the analytical solution of three benchmark problems involving solutions with shocks and kinks. For each of the numerical schemes used, we compute the L_2 error due to the discretization method, as a function of the number of grid points. The result is shown in Figure 1. This study leads to several conclusions. The Lax-Friedrichs scheme is very diffusive. Its behavior is very representative of linear schemes to approximate a hyperbolic PDE. Consequently, we do not think that it is a good idea to use linear numerical schemes to approximate the solution of the PDE, even if it would have the advantage of making the constraints linear in the resulting optimization program. The left centered scheme is less diffusive, but fails to capture the kinks of the solution. However, it still provides good L_2 convergence. The JST scheme captures shocks accurately because of its anti diffusive term, and thus gives the best results overall. It will be used for the rest of this study.[1] Note that capturing shocks is crucial: shocks represent the location of fronts of traffic jams, which we want to track.

III. NETWORK CONTROL VIA ADJOINT METHODS

Consider solving the following problem: maximize the throughput (i.e. flux of landing aircraft) at a destination airport, while maintaining the density of aircraft everywhere lower than a given threshold. Let us call $\rho_{max,i}$ the maximal allowed density on link i, $v_{max,i}(\cdot)$ and $v_{min,i}(\cdot)$ the maximal and minimal achievable speeds on link i (which can

---

[1]This validation is to the best of our knowledge the first which was actually implemented to assess the accuracy of the approximation as a function of the discretization size. Note also that confusion often arises between scale cell size (defined previously by Daganzo [8], i.e. line element) and discretization size (whose mathematical definition is available in [10]). These quantities are completely unrelated, as cell size is a physical length which pertains to the application (for example a portion of highway or jetway), whereas the discretization length is an arbitrary small length chosen between gridpoints such that the discretization will approximate the continuous problem accurately. Typically, a cell should contain at least a dozen grid points (in fact at least a hundred in the present simulations).
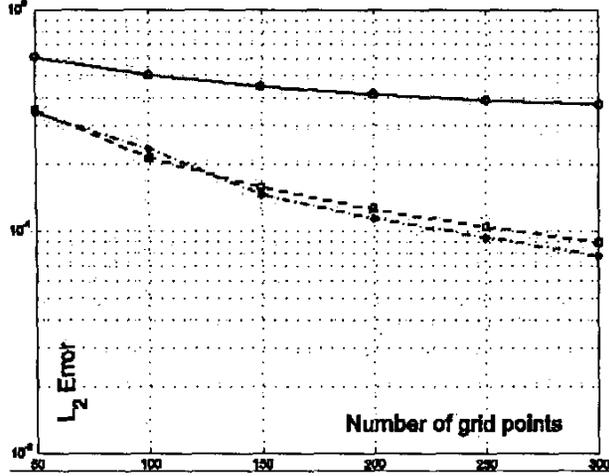
Fig. 1. L_2 error due to the discretization method, as a function of the number of grid points for both schemes. The analytical solution presented in [3] is used for this comparison. Lax-Friedrichs scheme (solid), Jameson-Schmidt-Turkel scheme (—·), left-centered scheme (- -).

depend on location). Using the notations of Section II, the optimization problem thus reads:

min: $-\sum_{i:i\in\mathcal{F}} \int_0^T \rho_i(L_i,t)v_i(L_i,t)\,dt$

s.t.: (1)

$$\rho_i(x_i,t) \le \rho_{\max,i}$$
$$\forall i \in \{1,\cdots,N\}, \forall x_i \in [0,L_i], \forall t \in [0,T] \quad (2)$$
$$v_{\min,i}(x_i) \le v_i(x_i) \le v_{\max,i}(x_i)$$
$$\forall i \in \{1,\cdots,N\}, \forall x_i \in [0,L_i], \forall t \in [0,T]$$
$$0 \le \beta_i(t) \le 1 \qquad \forall i \in \mathcal{D}, \forall t \in [0,T]$$

The difficulty posed by the constraints can be avoided in practice by using a classical optimization technique called *barrier* [6], in which the cost is augmented by a logarithmic term, which prohibits violation of the constraints.

min: $\mathcal{J} := -\sum_{i:i\in\mathcal{F}} \int_0^T \rho_i(L_i,t)v_i(L_i,t)\,dt$
$$\quad -\frac{1}{M}\sum_{i=1}^N \int_0^T \int_0^{L_i} \log((\rho_{\max} - \rho_i(x_i,t))\cdot$$
$$\quad (v_{\max} - v_i(x_i,t))(v_i(x_i,t) - v_{\min,i}))\,dx_i\,dt$$
$$\quad -\frac{1}{M}\sum_{i:i\in\mathcal{D}} \int_0^T \log(\beta_i(t)(1 - \beta_i(t)))\,dt$$

s.t.: (1)

$$\quad (3)$$

We call $H(v,\beta,\rho)$ the augmented cost function. When ρ, β and v are used without indices, it means that they are vectors, i.e. $v = [v_1,\cdots,v_N]$. Note that the two last constraints in the optimization program (2) have disappeared into the cost function. This constrained optimization problem is easier to solve in practice. It is asymptotically equivalent to the problem of interest when $M \to +\infty$. We use an adjoint method to algebraically compute the gradient of the cost function. This method was extensively [5] in flow control. We now adapt the adjoint method to the case in which we have a set of PDEs coupled through the boundary conditions, and subject to constraints. The adjoint method computes the gradient of the cost function $H(v,\beta,\rho)$ when ρ is an implicit function of v and β via the dynamics (1). Let

us denote $\mathcal{J}$ the cost function of the two variable v and β: $\mathcal{J} : (v,\beta) \to \mathcal{J}(v,\beta) = H(v,\beta,\rho)$ where ρ is the solution of the PDE system (1). We compute the linearized (1), which we will use to compute the gradient of the cost function in the optimization program (3). We denote by $'$ the linearized quantities around a nominal value denoted by $\bar{}$: $\rho_i = \bar{\rho}_i + \rho_i'$. We call $\mathcal{N}_i'(\cdot)$ the linearized LWR operator, and $q_i = \rho_i v_i$. In order to abbreviate the notation, we will write $q_i' = \rho_i'\bar{v}_i + \bar{\rho}_i v_i'$ and $\bar{q}_i = \bar{\rho}_i\bar{v}_i$. We omit the time and space dependence when they are obvious. We are NOT using Einstein's notations. The linearized (1) reads:

$$\begin{cases} \mathcal{N}_i'(\rho_i') := \mathcal{N}_i'\rho_i' = \frac{\partial\rho_i'}{\partial t} + \frac{\partial\rho_i'\bar{v}_i}{\partial x} = -\frac{\partial\bar{\rho}_i v_i'}{\partial x} \\ \qquad\qquad\qquad\qquad\qquad \forall i \in \{1,\cdots,N\} \\ \rho_i'(x,0) = 0 \qquad\qquad \forall i \in \{1,\cdots,N\} \\ q_i'(0,t) = \sum_{j\in\mathcal{U}(i)} q_j'(L_j,t) \qquad \forall i \in \mathcal{M} \\ q_{i_l}'(0,t) = \beta_i'(t)\bar{q}_i(L_i,t) + \bar{\beta}_i(t)q_i'(L_i,t) \quad (4) \\ \qquad\qquad\qquad\qquad\qquad \forall i \in \mathcal{D} \\ q_{i_r}'(0,t) = -\beta_i'(t)\bar{q}_i(L_i,t) + (1 - \bar{\beta}_i(t))q_i'(L_i,t) \\ \qquad\qquad\qquad\qquad\qquad \forall i \in \mathcal{D} \\ \rho_i'(0,t)\bar{v}_i(0) + \bar{\rho}_i(0,t)v_i'(0,t) = 0 \qquad \forall i \in \mathcal{S} \end{cases}$$

The first variation of $\mathcal{J}$ is obtained from (3):

$$\mathcal{J}' = -\sum_{i:i\in\mathcal{F}} \int_0^T \rho_i'(L_i,t)\bar{v}_i(L_i,t) + \bar{\rho}_i(L_i,t)v_i'(L_i,t)$$
$$\quad +\frac{1}{M}\sum_{i=1}^N \int_0^T\int_0^{L_i} \left(\frac{\rho_i'(x_i,t)}{\rho_{\max,i}-\bar{\rho}_i(x_i,t)} + \frac{v_i'(x_i,t)}{v_{\max,i}-\bar{v}_i(x_i,t)}\right.$$
$$\quad \left.-\frac{v_i'(x_i,t)}{\bar{v}_i(x_i,t)-v_{\min,i}}\right) dx_i\,dt$$
$$\quad +\frac{1}{M}\sum_{i:i\in\mathcal{D}} \int_0^T \left(\frac{\beta_i'(t)}{1-\bar{\beta}_i(t)} - \frac{\beta_i'(t)}{\bar{\beta}_i(t)}\right) dt$$
$$\quad (5)$$

An integration by parts leads to the following identity for any two functions ρ_i' and ρ_i^*.

$$\int_0^T\int_0^{L_i} \rho_i^*\mathcal{N}_i'\rho_i'\,dx_i dt$$
$$= \int_0^T [\rho_i^*\rho_i'\bar{v}_i]_0^{L_i}\,dt - \int_0^T\int_0^{L_i} \rho_i'\bar{v}_i\frac{\partial\rho_i^*}{\partial x_i}\,dt\,dx_i$$

which can be rewritten using the standard inner product denoted $\langle\cdot,\cdot\rangle_i$ for the domain $[0,L_i]\times[0,T]$:

$$\langle\rho_i^*|\mathcal{N}_i'\rho_i'\rangle_i = \langle\mathcal{N}_i^*\rho_i^*|\rho_i'\rangle_i + b_i \quad (6)$$

where $\begin{cases} \mathcal{N}_i^* = -\frac{\partial(.)}{\partial t} - \bar{v}_i\frac{\partial(.)}{\partial x_i} \\ b_i = \int_0^{L_i} [\rho_i^*\rho_i']_0^T\,dx_i + \int_0^T [\rho_i^*\rho_i'\bar{v}_i]_0^{L_i}\,dt \end{cases} \quad (7)$

We will denote by $\langle\cdot,\cdot\rangle_{[0,T]}$ the standard inner product in $[0,T]$. $\mathcal{N}_i^*$ is called the adjoint operator of $\mathcal{N}_i'$. In order to express the first variation of $\mathcal{J}$ as a function of the v_i' and β_i' only, we choose an adjoint density field ρ_i^* that cancels all the terms containing ρ_i' in the cost function. First, in order to eliminate the term $\frac{1}{M}\sum_{i=1}^N \int_0^T\int_0^{L_i} \frac{\rho_i'(x_i,t)}{\rho_{\max,i}-\bar{\rho}_i(x_i,t)}dx_i dt$, we choose ρ_i^* such that

$$\mathcal{N}_i^*\rho_i^* = \frac{1}{M(\rho_{\max,i}-\bar{\rho}_i)} \quad (8)$$

This is a first order linear hyperbolic PDE, which is well-posed if $\bar{\rho}_i$ is known and both the boundary conditions at one location and the initial conditions at one time are specified.
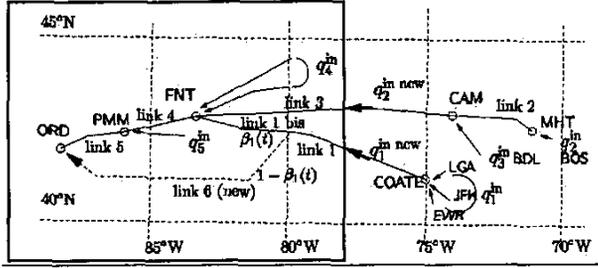
Fig. 2. Network model shown in [3]. We now add a divergence link in order to be able to show that we are able to control the density of aircraft by splitting the flow. For this simulation, we restrict ourselves to the box including ORD. The new additional link is shown with a dashed line. We call β_1 the portion of flow which stays on link 1 (called 1 bis) and $1 - \beta_1$ the portion which goes into the new link (link 6).

This allows us to enforce two other conditions for ρ_i^* in order to cancel all the terms containing ρ_i'. We can choose:

$$
\begin{cases}
\rho_i^*(x_i, T) = 0 & \forall i \in \{1, \cdots, N\}, \forall x_i \in [0, L_i] \\
\rho_i^*(L_i, t) = -1 & \forall i \in \mathcal{F}, \forall t \in [0, T] \\
\rho_i^*(0, t) = \rho_j^*(L_j, t) \forall i \in \mathcal{M}, \; \forall j \in \mathcal{U}(i), \; \forall t \in [0, T] \\
\rho_i^*(L_i, t) = \bar{\beta}_i(t)\rho_{i_j}^*(0) + (1 - \bar{\beta}_i(t))\rho_{i_r}^*(0) \\
\qquad\qquad\qquad\qquad \forall i \in \mathcal{D}, \forall t \in [0, T]
\end{cases}
$$
(9)

These conditions have been chosen by necessity of the algebraic derivation, in order to cancel appropriate terms in the perturbation of the cost function.[2] After some algebra, using (6–9), we are able to express the first variation $\mathcal{J}'$ of $\mathcal{J}$ as a function of the first variations control variables only (v_i' and β_i'), as well as nominal and adjoint quantities, which we can evaluate. The result reads:

$$
\begin{aligned}
\mathcal{J}' = \sum_{i=1}^{N} \left\langle \bar{\rho}_i \frac{\partial \rho_i^*}{\partial x_i} + \frac{1}{M} \left(\frac{1}{v_{\max,i} - \bar{v}_i} - \frac{1}{\bar{v}_i - v_{\min,i}} \right) \middle| v_i' \right\rangle_i \\
+ \sum_{i \in \mathcal{D}} \left\langle \bar{\rho}_i(L_i)\bar{v}_i(L_i)(\rho_{i_j}^*(0) - \rho_{i_r}^*(0)) + \frac{1}{M}(\frac{1}{1-\bar{\beta}_i} - \frac{1}{\bar{\beta}_i}) \middle| \beta_i' \right\rangle_{[0,T]}
\end{aligned}
$$

where again $\langle \cdot, \cdot \rangle_i$ denotes the inner product for the domain $[0, L_i] \times [0, T]$ and $\langle \cdot, \cdot \rangle_{[0,T]}$ for $[0, T]$. The functions $v_i(\cdot, \cdot)$ and $\beta_i(\cdot)$ generated by this method might be ill-behaved and thus be inappropriate for practical Air Traffic Control applications. We can alleviate this difficulty by projecting the descent direction $\bar{\rho}_i \frac{\partial \rho_i^*}{\partial x_i} + 1/M(1/(v_{\max,i} - \bar{v}_i) - 1/(\bar{v}_i - v_{\min,i}))$ into a vector space $\mathcal{E}$ of appropriate functions, for example the set of continuous functions with bounded derivative, or the set of continuous piecewise affine functions.

[2] The algebra which led to the "good choice" (9) is available from the authors upon request. In addition, a physical interpretation of the boundary and terminal conditions of the adjoint can be given. The first condition is terminal and stipulates that the sensitivity of the solution to perturbations of the system at $t = T$ is zero. The second conditions accounts for the sensitivity of the solution at the sink: by actuating directly there, one decreases the objective function. The third condition at every merging node says that the sensitivity is the same for all branches connected to the node, at that point. The last condition says the same at the diverging nodes, weighted by the mean $\bar{\beta}_i$ which represents the portion of flow choosing the respective links outgoing from the node.

IV. APPLICATION TO CONTROLLER DESIGN

In this section, we demonstrate the effectiveness of the method by applying it to the air traffic model built in [3]. Please refer to [3] for a description of airspace. Figure 2 shows the area which we will control (enclosed by a box). The inflows into the box are thus now $q_1^{\text{in new}}$ and $q_2^{\text{in new}}$ as shown in Figure 2. We want to impose the following constraint: for all links, the density should be below a threshold $\rho_{\max}$ which we impose. We allow the flow to be split into a new link (link 6), in order to aid satisfaction of the maximal density constraints. We call β_1 the corresponding split factor: β_1 is the fraction of the flow which stays on link 1 (called 1 bis); $1 - \beta_1$ is the fraction which is routed through link 6. This new link might use another arrival into the airport (it enters the arrival airspace from an other direction).[3] We simulate the following three scenarios:

Scenario 1: normal traffic. (Real data) We take ETMS data, from which we extract initial conditions and inflows, as explained in [3]. We impose a restriction on the density and control the flow.

Scenario 2: heavy traffic. (Modified real data) We take the same data as for the previous case, and add additional aircraft in order to overload even more the network.

Scenario 3: congested network. We generate data with very high densities of aircraft. This situation does not use ETMS data; it is generated randomly.

Figure 3 shows the decrease in cost for the three scenarios as a function of the total number of iterations (i.e. iterations on M and gradient advances). As can be seen in this Figure, the more congested the situation is, the higher the cost is. The evolution of the cost with iterations exhibits two distinct behaviors, as often with barrier methods [6]: large jumps corresponding to the increases in M, and shallower decreases corresponding to the gradient advances. Convergence is clearly observed for the three scenarios. We display some of the results for the third case. An animation (in form of an .avi movie file) corresponding to each of the three scenarios is available at [18]. We now describe in detail the scenario corresponding to Case 3. We run a one hour simulation. Figure 3 shows the aircraft density on all links at various instants, in the absence of control: the velocity is the mean velocity profile determined for each link in [3], and no aircraft is allowed into link 6 (i.e. $\beta_1 = 1$). The initial density is shown in the top left corner. The inflow into links 1 and 3 is such that at time $t = 27$, the density threshold (represented by the horizontal line on each subplot) is violated until time $t = 45$. At time $t = 55$, it is violated again, until the end of the experiments. Figure 4 shows the same experiment when link 6 is now opened to traffic, and velocity control is enabled. As can be seen, about half of the

[3] Note that using β_1 is equivalent to using turning proportions in road traffic, and might not be the best way to represent network traffic. It could be better to define an assignment proportion, i.e a coefficient indexed by destination. This might be implemented in the future (as a part of the control strategy), using a framework such as the one developed by Papageorgiou [17].
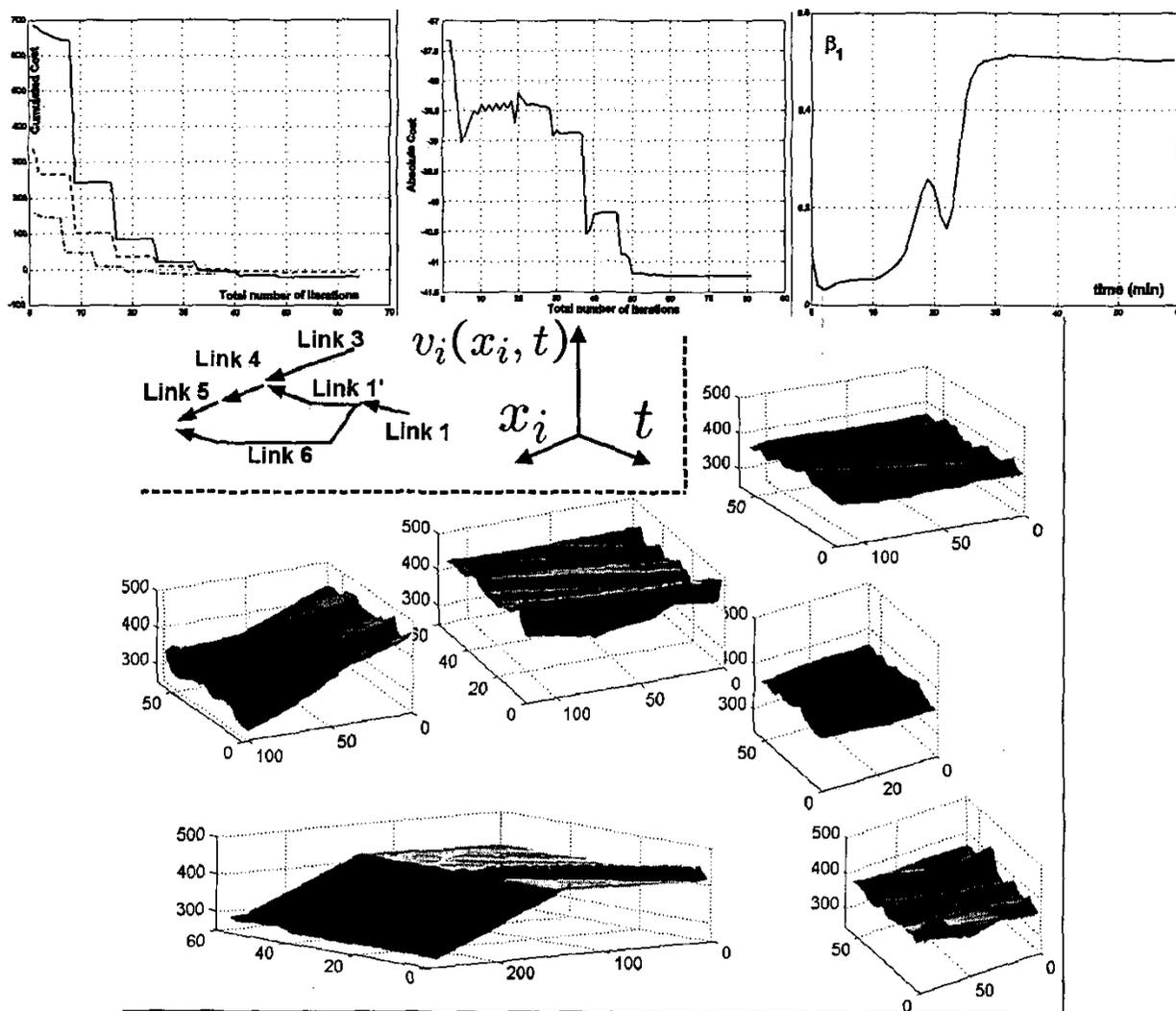
Fig. 3. **Top left:** Decrease of the cost as a function of the iterations for the three scenarios. The increases in M are clearly visible (steps), while the gradient descent is more subtle. Congested traffic (solid); heavy traffic (- -); normal traffic (—·). **Top middle:** Decrease of the true cost as a function of the iterations. The true cost is the cost $\mathcal{J}$ without the barrier terms. The method does not guarantee the monotonicity of the decrease but only the convergence. **Top right:** Evolution of the β_1 parameter as a function of time. **Bottom:** Evolution of the velocity fields as a function of time for the different links. Each of the plots corresponds to a link, (see top left corner). The axis of each subplot are: x_i (arclength along the link), t (time) and $v_i(x_i, t)$, the velocity distribution.

traffic incoming into link 1 is rerouted into link 6, and the other half into link 1 bis. Figure 3 shows the variation of β_1 with time. As can be seen, around $t = 20$ min., there is a peak of about 25% of aircraft routed into link 6, which settles to 50% at $t = 30$. The routing control enables avoidance of violation of maximal density shown in Figure 4. The first violation is avoided by velocity changes.

The velocity profiles $v_i(x_i, t)$ are shown in Figure 3. Each of the subplots corresponds to one of the links. For links 5 and 6, one can clearly see the descent velocity profiles. Also, for link 6 (subfigure below), one can see a ridge. It corresponds to a set of aircraft which have to fly at high

speed into the airport. One can also see similar ridges on the other subplots, which have the same interpretation. For any ridge, the Controller command could be to the corresponding set of aircraft: "fly direct at 420 kts direct into [the next waypoint]". Note that in the absence of control, the first violation of the aircraft density threshold occurs 33 minutes after the beginning of the experiment, almost at the end of the network, which is not intuitive. This shows the efficiency of the method, which is capable of generating the right routing and speed assignments to prevent undesirable events from happening much later. Finally, the simulations are also depicted on a US map in Figure 5 using the same density
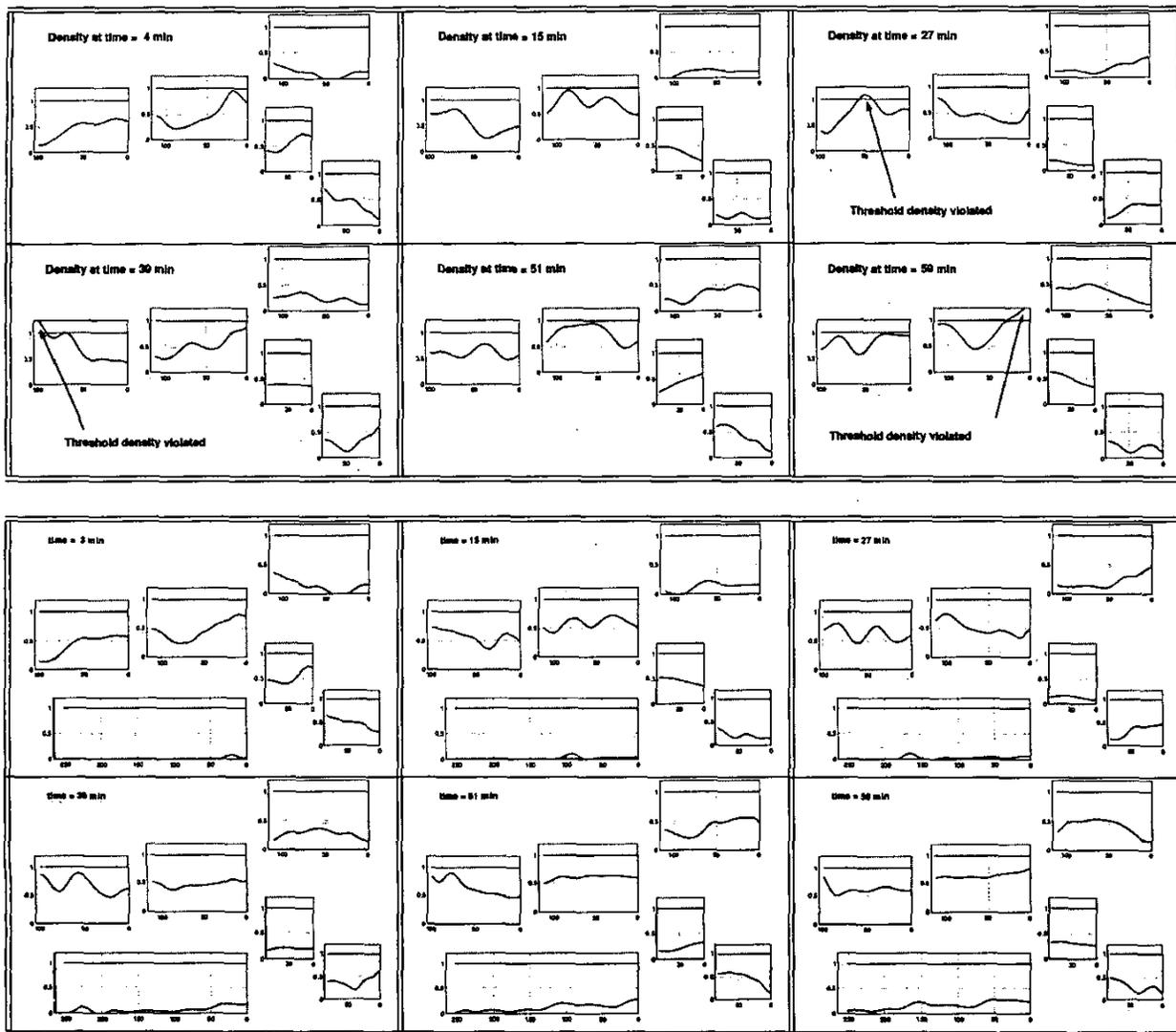
Fig. 4. **Top 6 subfigures:** Evolution of the aircraft density on the different links in the absence of control. Each of the subplot shows the density distribution at a given time on the corresponding link as in Figure 3 (the horizontal coordinate represents location, the vertical represents density). The horizontal line represents the density threshold (all quantities are nondimensionalized by ρ_{max}, so that the threshold density is 1). As can be seen, the density threshold is violated in link 5 at $t = 27$, $t = 39$ and $t = 59$. **Bottom 6 subfigures:** Evolution of the aircraft density with control applied. Note that link 6 is now open, and used. This prevents the second violation of density threshold observed in Figure 4 ($t = 59$): some of the flow is directly routed from link 1 to link 6. The first violation seen in the top 6 subfigures is avoided by speed changes. This figure is also available in form of a .avi file at [18].

encoding as in [3]. One can see that before $t = 27$, all aircraft choose the direct route through link 5 to Chicago (it is shorter). After $t = 27$, the excessive amount of flow incoming into links 1 and 3 forces the flow to be split through links 1 bis and 6.

REFERENCES

[1] O. M. AAMO and M. KRSTIC. *Flow Control by Feedback.* Springer-Verlag, 2002.

[2] B. BAMIEH, F. PAGANINI, and M. A. DALEH. Distributed control of spatially-invariant systems. *IEEE Transactions on Automatic Control,* 47(7):1091–1107, 2002.

[3] A. M. BAYEN, R. RAFFARD, and C. J. TOMLIN. Eulerian network model of air traffic flow in congested areas. June 2004.

[4] A. M. BAYEN, R. RAFFARD, and C. J. TOMLIN. Hybrid control of PDE driven highway networks. LNCS. Springer Verlag, 2004.

[5] T. R. BEWLEY. Flow control: new challenges for a new renaissance. *Progress in Aerospace Science,* 37:21–58, 2001.
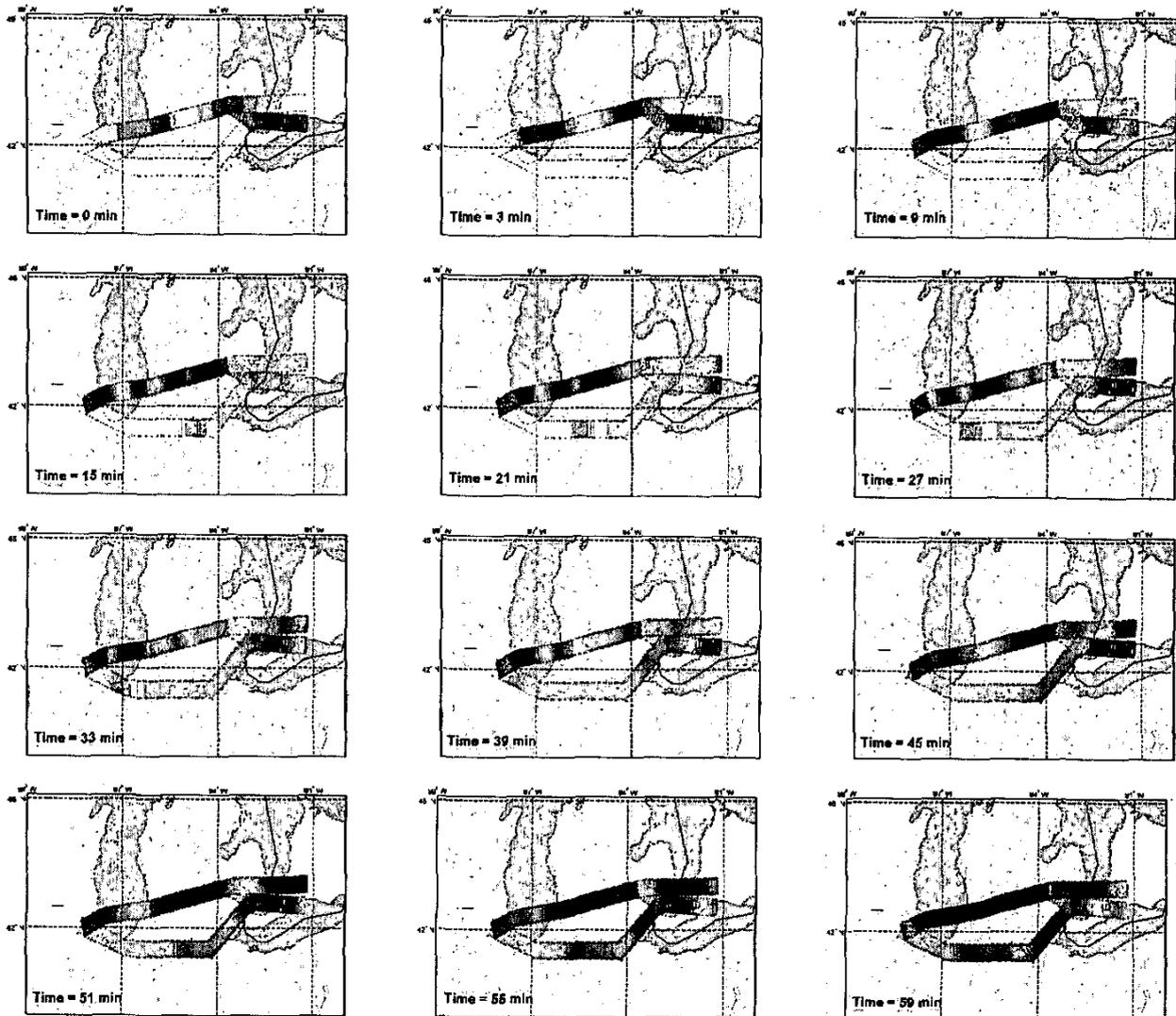
Fig. 5. Aircraft density in the network around Chicago in presence of control and velocity assignment. The density of the links is depicted by the color. The colored rectangles shown in this plot represent the density. The colorscale is: white for zero density; black for highest density. As can be seen and was shown in Figures 4, a good portion of the flow is routed into link 6 starting at time $t = 51$.

[6] S. BOYD and L. VANDENBERGHE. *Convex Optimization.* Cambridge University Press, To appear 2004.

[7] P. D. CHRISTOFIDES. *Nonlinear and robust control of PDE systems.* Birkhäuser, 2001.

[8] C. DAGANZO. The cell transmission model, part II: network traffic. *Transportation Research*, 29B(2):79–93, 1995.

[9] C. DAGANZO. A finite difference approximation of the kinematic wave model of traffic flow. *Transportation Research*, 29B(4):261–276, 1995.

[10] C. HIRSCH. *Numerical Computation of Internal and External Flows.* John Wiley & and Sons, 1988.

[11] A. JAMESON. Aerodynamic design via control theory. *Journal of Scientific Computing*, 3(3):233–260, 1988.

[12] A. JAMESON. Analysis and design of numerical schemes for gas dynamics 1: Artificial diffusion, upwind biasing, limiters and their effect on accuracy and multigrid convergence. *International Journal of Computational Fluid Dynamics*, 4:171–218, 1995.

[13] O. I. KOROLEVA and M. KRSTIĆ. Averaging analysis of periodically forced fluid flow networks. Submitted to *Automatica*, Sep. 2003.

[14] X. LITRICO. Robust IMC flow control of SIMO dam-river open-channel systems. *IEEE Transactions on Control Systems Technology*, 10(5):432–437, 2002.

[15] P. K. MENON, G. D. SWERIDUK, and K. BILIMORIA. A new approach for modeling, analysis and control of air traffic flow. In *Proceedings of the AIAA Conference on Guidance, Navigation and Control*, Monterey, CA, Aug. 2002. Paper 2002-5012.

[16] L. MUNOZ, X. SUN, R. HOROWITZ, and L. ALVAREZ. Traffic density estimation with the cell transmission model. In *Proceedings of the American Control Conference*, Denver, CO, June 2003.

[17] M. PAPAGEORGIOU. Dynamic modeling, assignment, and route guidance in traffic networks. *Transport. Res.*, B-24:471–495, 1990.

[18] http://cherokee.stanford.edu/~bayen/ACC04.html.